Surface chemistry and reactivity of skin-passed hot dip galvanized coating

Jean-Michel Mataigne, Véronique Vaché, Monique Repoux

J.-M. Mataigne (ArcelorMittal, Research Automotive Products, Maizières-les-Metz)
V. Vaché (Novelis, Foil Innovation Center, Belvaux)
M. Repoux (Ecole des Mines de Paris, CEMEF Sophia-Antipolis)

Surface chemistry and reactivity of skin-passed hot dip galvanized coating

This paper aims at describing surface chemistry and reactivity of skin-passed hot dip galvanized coatings.
GI coatings surfaces are covered by a very thin aluminum oxide 5 nm thick layer that precipitates just immediately after wiping.
Anisotropic growing of zinc crystals during solidification induces a strong basal texture in GI coatings. Metallic aluminum is rejected in the last liquid during solidification, and so accumulates along zinc grain boundaries and close to the free surface.
Skin-pass induced changes in GI coating surface chemistry, crystallography and reactivity have been assessed. Local coating analyses have been performed (XPS, TOF-SIMS) in order to describe local effects of roughness indentation during skin-pass on coating characteristics.
A laboratory bi-crushing device has been used on not skin-passed GI coatings, in order to reproduce on large scales heavy deformations that exist locally when skin-pass roll roughness peaks indent the coating.
Such a protocol allowed analyzing the way aluminum oxide is crushed down in the zinc coating during deformation, then re-build during ageing.
XRD and EBSD experiments have been conducted illustrating zinc textures changes induced by deformation.
Reactivity of such surfaces has been tested using probe molecules, like fatty acids.

INTRODUCTION

For about twenty years, GI (galvanized) coating has been increasingly used for the construction of automotive bodies, particularly in Western Europe. The very demanding automotive market is asking for a perfect mastering of GI coating surface behavior when stamping, assembling, phosphating and painting *(1, 2)*.

This paper aims at providing an up-dated knowledge of GI coating surface states, which should be useful for understanding GI behavior during the different operations performed in the making of cars.

SAMPLING

Samples have been taken from a GI line (GI bath with 0.2 wt% Al), either before or after skin-pass. Some non skin-pass samples have been skin-passed at the laboratory scale, while others have undergone bi-crushing deformations. *Table I* presents the samples used in this study, with their ratios of plateaus, inter-plateaus and valleys as defined in *figure 1*.

TABLE I: Sampling.

Samples	State	% plateaus	% inter-plateaus	% valleys	Ra0,8 (µm)
NSK	Without skin-pass				0.16
SK - A	Lab EBT skin 1% Elong.	30	17	53	4.3
SK - B	Lab EBT skin 1% Elong.	11	61	28	0.9
SK - C	Indus. EBT skin 1% Elong.	28	34	38	0.8
SK - D	Indus. EBT skin 1% Elong.	58	0	42	1.9

Subject of a presentation at the 7th International Conference on Zinc and Zinc Alloy Coated Steel Sheet (Galvatech'07), ISIJ, Osaka, Japan, November 19-22, 2007.

Article available at http://www.revue-metallurgie.org or http://dx.doi.org/10.1051/metal/2009013

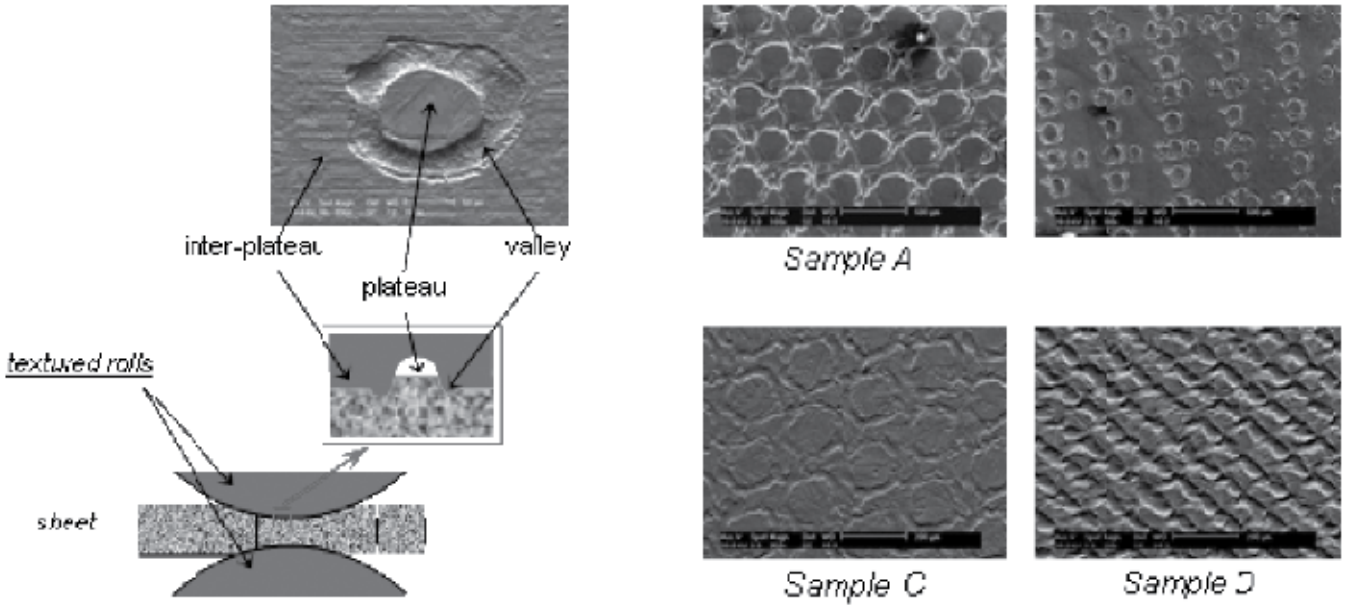

Fig. 1 - Sketch of roughness indentation during skin-pass, with definition of "inter-plateaus", "plateaus" and "valleys" areas and SEM pictures of skin-passed samples.

SURFACE CHEMISTRY AND ZINC GRAINS TEXTURE BEFORE SKIN-PASS

GI coatings are produced using a molten zinc bath (460 °C) containing 0.2 wt% Al at least. Such a bath chemical composition gives rise to the precipitation of the $Fe_2Al_5(Zn)$ inter-metallic compound on the steel surface.

That very rapid reaction lasts about 0.2 seconds and inhibits further reaction between iron and zinc *(3)*. The so-called inhibiting layer is too thin (about 0.15 µm) to be observed on a cross section using an optical microscope but can easily be characterized, from the top, under SEM, provided the zinc coating has been first chemically removed *(fig. 2)*.

Sub-microscopic Fe_2Al_5 crystals are fully covering the steel surface, and their size and shape are dependent on the orientation of underlying steel grains.

Liquid zinc is then dragged out from the bath by the withdrawing strip and finally wiped by air knives. Solidification then occurs a few seconds later. The Al content of the dragged liquid zinc is about the same as the one in the bath. For a 10 µm thick GI coating, produced with a 0.2 wt% Al bearing zinc bath, chemical

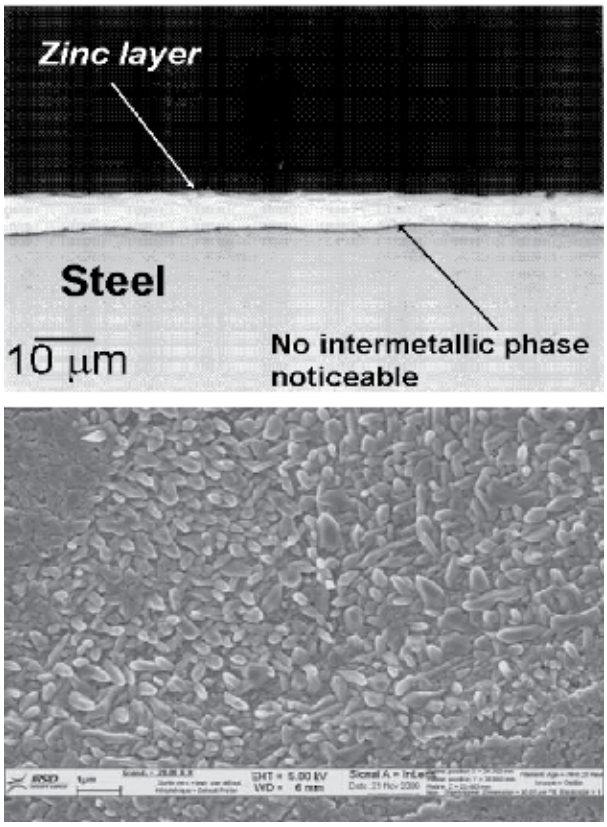

Fig. 2 - Optical cross section of GI coating (up); inhibiting layer as observed from the top, under SEM, after chemical stripping of the zinc layer (low).

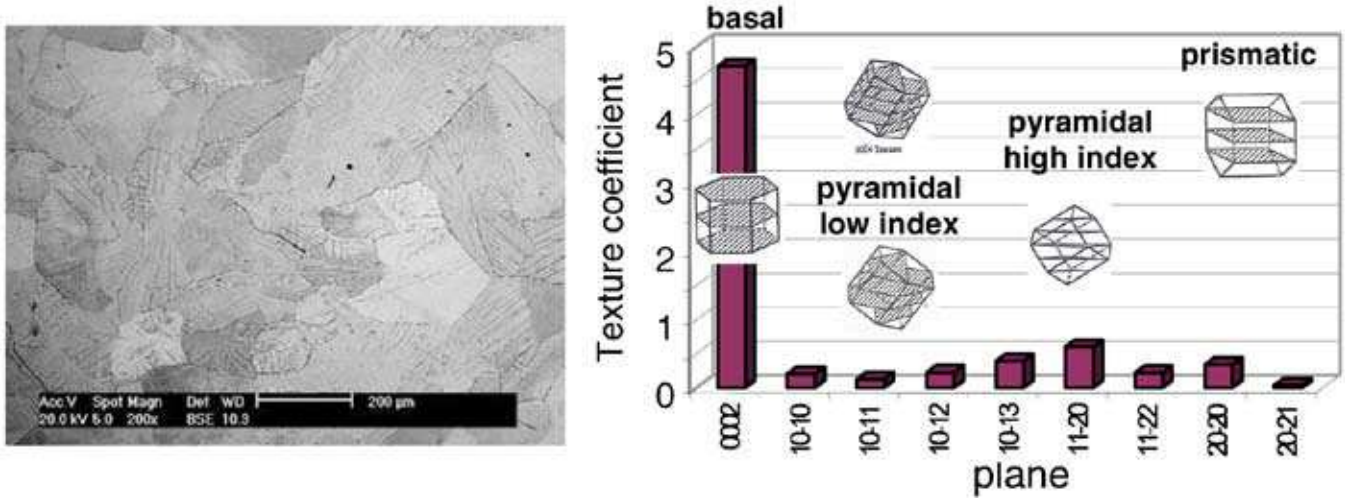

Fig. 3 - SEM picture of NSK GI coating surface (left); Relative Texture Coefficient (RTC) of NSK GI coating, calculated by comparing XRD intensities recorded on coating to the ones recorded on zinc powder (right).

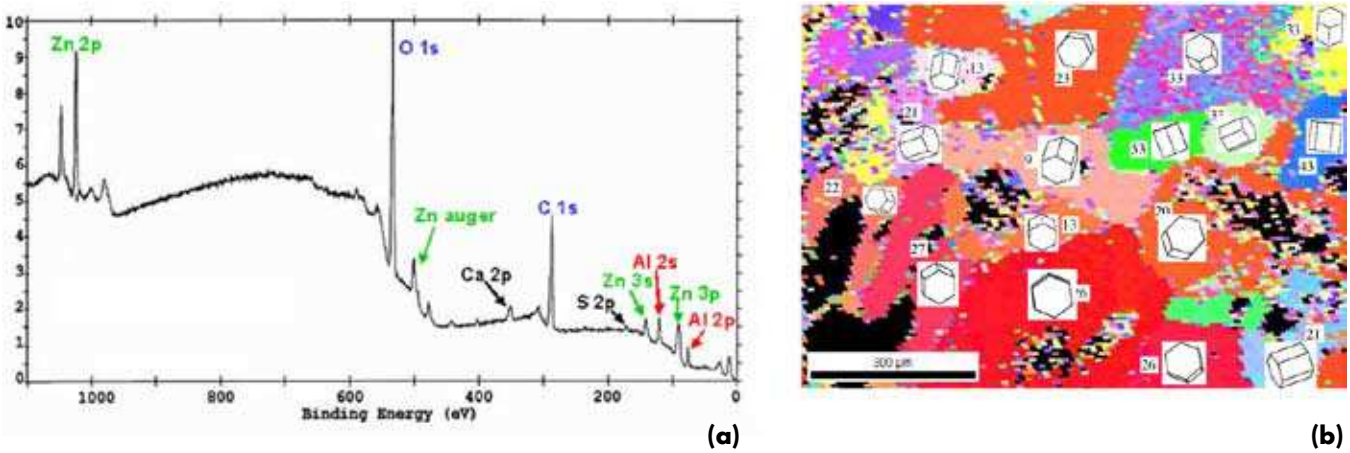

Fig. 4 - XPS spectrum recorded on NSK sample on the left and inverse pole figure from EBSD measurements on the right; local TOF-SIMS $^{27}Al/^{64}Zn$ ratios are also provided for each zinc grain.

analysis shows that about half of the total aluminum in the coating is located within the inhibition layer, the other half being located in the zinc layer, so that the total amount of Al in the coating is about 0.4 wt%.

GI coating solidifies into large grains of about 300 to 400 µm, much larger than the coating thickness, developing a very strong basal texture *(4) (fig.3)*.

Zinc coating microstructure after solidification is dependent on the nucleation mechanisms of solid zinc into liquid coating, which is still a matter of research. The real nucleation law remains unknown up to now, but one can think that the development of large zinc grains exhibiting a basal orientation is related to the very rapid growth of solid zinc nuclei along basal planes as compared to the very slow solidification rate along the c axis. All nuclei oriented with the c axis perpendicular to the steel surface will grow easily without being limited by the free surface neither by the steel/coating interface. If that mechanism prevails, nucleation can be random and basal texture is expected to get stronger with thinner coating weight, but there is still no evidence of that. On the contrary, zinc grains centers, i.e. zinc nuclei, are frequently observed on the steel/coating interface side, and it is so conceivable that the nucleation law is not random.

Wiping induces precipitation of an Al rich oxide film on top of the liquid coating, which protects the liquid from further oxidation *(5, 6)*. During solidification, Al is segregated into the last liquid, particularly along the free surface. Despite this Al segregation along the surface, the Al rich oxide film remains very thin, less than 5 nm and act as a passive layer. XPS spectra recorded on such surfaces *(fig. 4 a)* are related to depths ranging

TABLE II: Semi-quantitative surface chemistry from XPS analysis recorded on NSK sample.

at. %	Al	Zn	C	O	Al/Zn Atomic ratio
NSK	16 ± 2	8 ± 0.5	28 ± 2	48 ± 2	2 ± 0.4

from 2 nm (Zn 2p peak) down to 6 nm (Al 2p peak). Only oxidized forms of Al are detected while Zn Auger peak reveals the presence of both oxidized and metallic states of Zn. Semi-quantitative analysis of XPS results is presented in *table II*. Al atoms are about twice more numerous on the coating surface than Zn atoms.

Surface chemistry has also been measured by TOF-SIMS, recording positive ions. Sensitive factors being unknown, only normalized intensities ($^{27}Al/^{64}Zn$) are presented.

Combined local EBSD and TOF-SIMS measurements allowed correlating Al surface enrichment as recorded by TOF-SIMS with local zinc grain orientation *(fig. 4b)*.

The Al/Zn ratio is dependent on the zinc grain orientation: higher Al/Zn ratios corresponding to prismatic grains (from 35 to 40), intermediate ones to basal grains (close to 26) and lowest ones to pyramidal grains (from 9 to 20).

SURFACE CHEMISTRY AND ZINC GRAINS TEXTURE AFTER SKIN-PASS

Skin-pass operation induces a decrease of the basal texture *(table III)*. *Figure 5* points out the possible recrystallisation of zinc in areas deeply indented by roll roughness peaks.

EBSD experiments have been conducted allowing determining crystal orientation of individual zinc grains.

Table IV summarizes these results by presenting the average ratio of basal grains in each area. Strong basal orientation is only kept on plateaus, while inter-plateaus underwent intense twinning.

The weighted of EBSD values, computed for the entire sheet, is in good agreement with XRD measurements.

TABLE III: Relative texture coefficient as recorded by XRD.

	Basal	Low angle	High angle	Prismatic
NSK	86	1	6	7
Sample A	74	8	11	7
Sample B	50	14	20	16
Sample C	71	8	11	10
Sample D	65	15	13	7

TABLE IV: Ratios of basal grains of plateaus, inter-plateaus and valleys area of sample B.

Areas of sample B	% of basal grains
Plateaus (11% of the total surface area)	96 ± 1
Inter-plateaus (61%)	56 ± 4
Valleys (28%)	30 ± 1
% basal for the entire sheet (EBSD results)	53 ± 4
XRD – RTC Results	54 ± 4

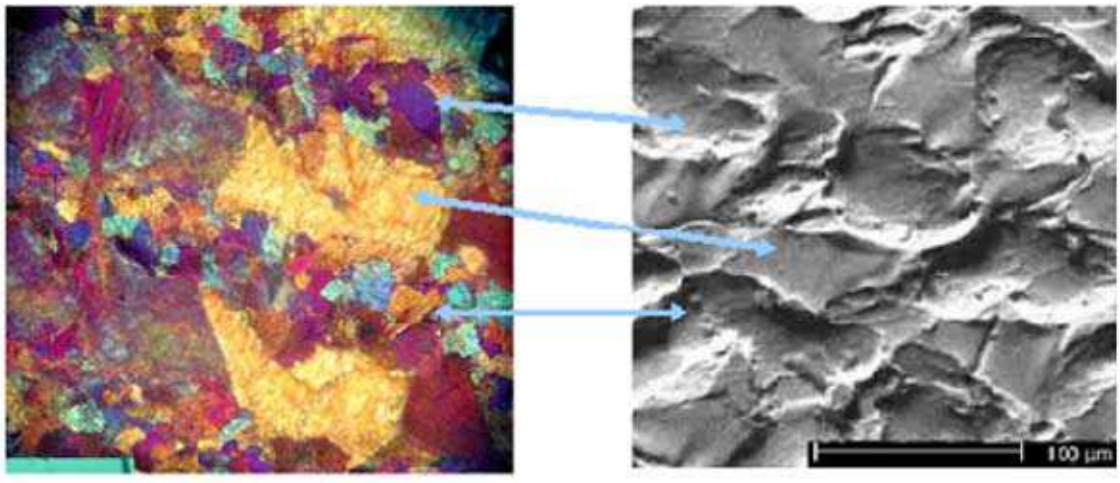

Fig. 5 - Polarized light optical (left) and SEM (right) micrographs of sample D surface.

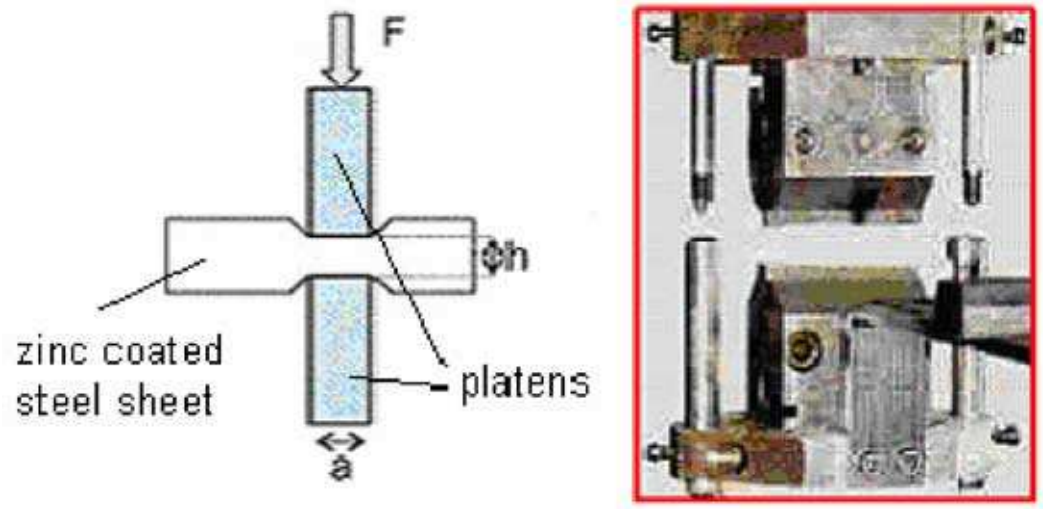

Fig. 6 - Sketch and photograph of the bi-crushing device.

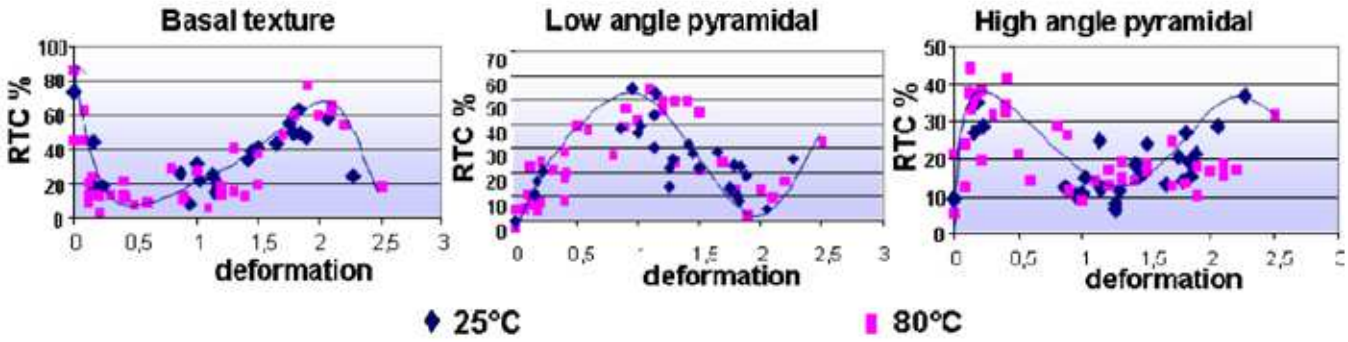

Fig. 7 - RTC of NSK sample as a function of plane-strain deformation rate.

EFFECT OF PLANE-STRAIN COMPRESSION

Bi-crushing device *(fig. 6)* has been developed in order to reproduce deformations locally induced by the skin-pass on larger surfaces.

Samples thicknesses are measured before (ei) and after (ef), the plane-strain compression test and the sheet deformation is given by:

$$\varepsilon = \frac{2}{\sqrt{3}} \ln\left(\frac{ei}{ef}\right)$$

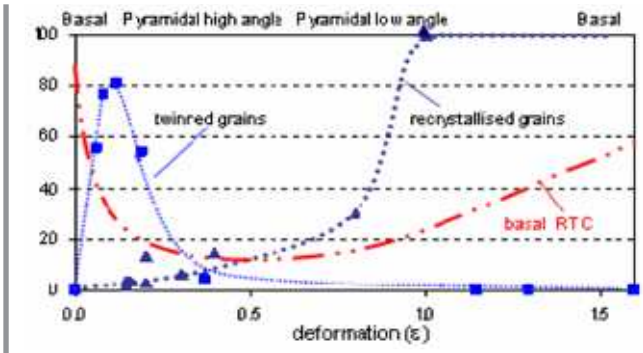

Fig. 8 - Rates of twinned and recristallized Zn grains as a function of plane-strain deformation rate (sample NSK).

Figure 7 represents the texture evolution induced by plane-strain compression. The texture evolves from basal to high angle pyramidal for deformation ranging from 0.1 to 0.4, then to low angle pyramidal with deformation close to 1, then basal again for deformation of about 2 and high angle pyramidal again.

With small deformations, intense twinning of basal grains occurs first *(fig. 8)*. Maximum twinning is reached when ε is equal to 0.1. Recrystallisation starts after twinning and texture evolves from high angle to low angle pyramidal first, basal next, corresponding to re-alignment of c-axis parallel to the compression direction (re-alignment of densest atomic planes perpendicularly to the compression direction).

It can be deduced from these results that deformation in the inter-plateaus areas of a skin-passed sample is close to 0.1 while it can be close to 1 in valleys areas.

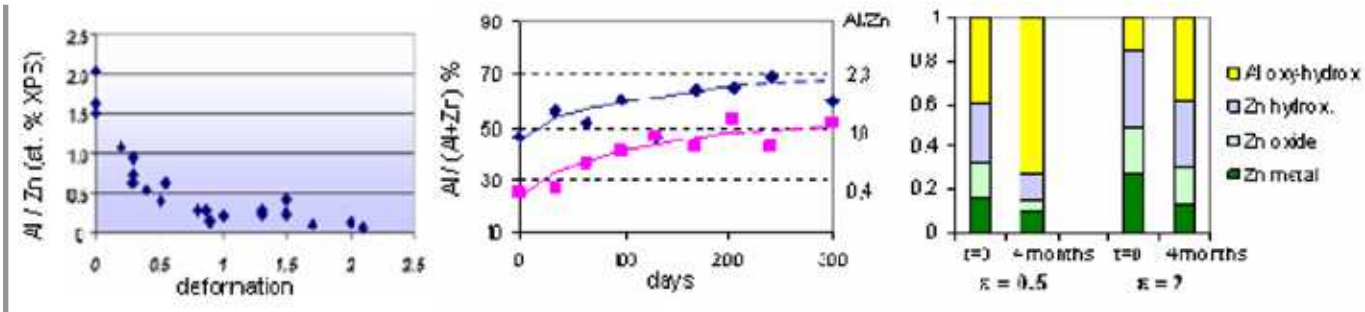

Fig. 9 – Al/Zn XPS ratio as a function of deformation on the left, after ageing for two ε levels on the centre, and Al oxide rebuilding at the expenses of Zn oxide and hydroxide on the right.

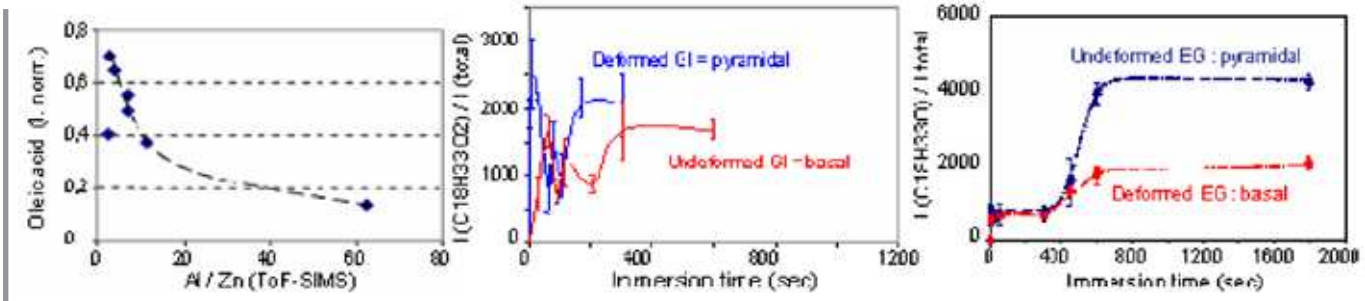

Fig. 10 – Tof-SIMS oleic acid peak as a function of surface Al on the left (immersion time: 600 s), and as a function of immersion time for un-deformed and deformed GI coating (centre) and EG coating (right). The solution was 1% oleic acid in hexadecane.

AGEING AFTER PLANE-STRAIN COMPRESSION

Al oxide layer is crushed down during plane-strain compression (*fig. 9*). Ageing during storage after plane-strain compression, has been measured. Samples were oiled then stored just after the compression test.

Figure 9 shows a rapid Al oxide re-building during storage for samples having undergone small deformations (high angle pyramidal texture) and a slower one for heavier deformation rates.

High resolution XPS measurements suggest the following mechanisms explaining Al oxide re-building: metallic Zn atoms, exposed to air during deformation, are immediately oxidized and hydroxydized, metallic Al diffuses during ageing toward the free surface to reduce Zn oxides and hydroxides.

SURFACE REACTVITY WITH A FATTY ACID

Thanks to the plane-strain compression test, samples with varying surface Al and crystal textures where immerged into oleic acid solution. Zn-oleates and de-hydrogenated oleic acid molecules were further detected with the help of TOF-SIMS. *Figure 10* shows that GI reactivity with oleic acid is reduced by the presence of surface Al and enhanced when the texture is pyramidal. Same experiments performed on an electro-galvanized sample (EG), with no surface Al, exhibiting a pyramidal texture in the un-deformed condition and a basal one after deformation confirmed that result.

CONCLUSION

XPS, TOF-SIMS, XRD and EBSD experiments have been conducted on GI coatings, having undergone either skin-pass, either plane-strain compression tests.

Main conclusions are as follows:

- GI coatings are covered by a very thin Al oxide film nucleating during wiping and exhibit a very strong basal texture after solidification;
- Skin-pass operation induces crushing of Al oxide film and strong Zn grains texture evolution starting by twinning for small deformation; heavier deformation can also induce Zn grains recrystallisation;
- Ageing during storage allows the repair of surface Al oxide, particularly in areas having undergone intermediate deformation rates;
- Oleic acid chemi-sorption is enhanced with the removal of surface Al and the development of pyramidal textures.

REFERENCES

(1) *(D.) QUANTIN, (M.) BABBIT - Proc.of Galvatech'98, Chiba, 583, 1998.*

(2) *(J.-M.) MATAIGNE - SAE 2001 World Congress, Detroit, paper 0077, 2001.*

(3) *(J.-M.) MATAIGNE - Key mechanisms in galvanizing of steel sheet, Proc of Galvatech'07, Osaka, 2007.*

(4) *(C.) MAEDA, (H.) FUJISAWA, (J.) SHINOMURA, (M.) KONISHI - Proc.of Galvatech'98, Chiba, 1998.*

(5) *(M.) DUBOIS - Proc.of Galvatech'01, Bruxelles, 2001.*

(6) *(V.) LEROY, (B.) SCMITZ - **Scandinavian Journal of Metallurgy**, 17, 1998.*